Drawing 3-Polytopes with Good Vertex Resolution*

André Schulz **

MIT, Computer Science and Artificial Intelligence Laboratory, Cambridge, USA,
schulz@csail.mit.edu.

Abstract. We study the problem how to obtain a small drawing of a 3-polytope with Euclidean distance between any two points at least 1. The problem can be reduced to a one-dimensional problem, since it is sufficient to guarantee distinct integer x-coordinates. We develop an algorithm that yields an embedding with the desired property such that the polytope is contained in a $2(n-2) \times 2 \times 1$ box. The constructed embedding can be scaled to a grid embedding whose x-coordinates are contained in $[0, 2(n-2)]$. Furthermore, the point set of the embedding has a small spread, which differs from the best possible spread only by a multiplicative constant.

1 Introduction

Let G be a 3-connected planar graph with n vertices $v_1, \ldots, v_n$ and edge set E. Due to Steinitz' seminal theorem [18] we know that G admits a realization as 3-polytope, and every edge graph of a 3-polytope is planar and 3-connected. The question arises how one can obtain a "nice" realization of a 3-polytope when its graph is given. One particular property, which is often desired from an aesthetically point of view, is that the vertices of the embedding should be evenly distributed. If two vertices lie too close together they are hard to distinguish. Such an embedding may appear as bad "illustration" for the human eye. Of course we can always scale a 3-polytope to increase all of its pointwise distances, but this does not affect the relative distances and the subjective perception of the viewer remains unchanged. Therefore, we restrict ourselves to an embedding, whose vertices have, pairwise, an Euclidean distance of at least 1. We say that in this case the embedding/drawing is under the *vertex resolution rule*. See [1] for a short discussion on resolution rules. Notice, that the resolution rule depends on a particular distance measure. Throughout the paper we use the Euclidean distance, but our results can be easily modified for the L_1 distance.

In 2d, drawings of planar graphs can be realized on an $O(n) \times O(n)$ grid [14,5]. Since the grid is small, these grid embeddings give a good vertex resolution for free. The situation for 3-polytopes is different. The best known algorithm uses a grid of size $O(2^{7.55n})$ [12]. Thus, the induced resolution might be bad for this grid embedding.

Let us briefly discuss some approaches for realizing G as 3-polytope. Steinitz' original proof is based on a transformation of G to the graph of the tetrahedron.

The transformation consists of a sequence of local modifications that preserve the realizability of G as 3-polytope. However, the proof does not include a direct method how to construct the 3-polytope given by G. The Koebe-Andreev-Thurston Theorem on circle packings gives a more constructive proof of Steinitz' Theorem (see for example Schramm [15]). This approach relies on non-linear methods which makes many geometric features of the constructed 3-polytope intractable. A third approach uses liftings of planar graphs with equilibrium stresses (known as the Maxwell-Cremona correspondence [20]). This powerful method is used in a series of embedding algorithms: Eades and Gravan [6], Richter-Gebert [13], Chrobak, Goodrich, and Tamassia [1], Ribó Mor, Rote, and Schulz [12]. A completely different approach is due to Das and Goodrich [4]. It uses an incremental technique which only needs $O(n)$ arithmetic operations for embedding G as 3-polytope, but works only for triangulated planar graphs.

Results: We show how to obtain an embedding of G as 3-polytope inside a $2(n-2) \times 2 \times 1$ box under the vertex resolution rule. It is even possible to make the box arbitrarily flat such that its volume gets arbitrarily small. But for aesthetic reasons we leave the side lengths at least 1. Our algorithm is based on the Maxwell-Cremona approach and extends the ideas of [12]. In contrast to the construction of [12] we can handle more complicated interior edge weights (stresses). Our algorithm creates an embedding with two more interesting properties: (1) it can be scaled to a grid embedding whose x-coordinates are in $[0, 2(n-2)]$, and (2) the point set of the embedding has a good ratio between its largest and shortest pointwise distance. We show that this number differs only by a constant from the best possible ratio.

Related work: In [1] Chrobak, Goodrich, and Tamassia introduced an algorithm that embeds a 3-polytope with good vertex resolution. However, their result was only published as preliminary version, without giving all details. Moreover, their algorithm is only applicable for polytopes that contain a triangular face. We reuse some of their ideas, but especially the complicated setting where the polytope does not have a triangular face requires completely new techniques.

2   Preliminaries: Maxwell and Tutte

Since G is 3-connected and planar, the facial structure of G is uniquely determined [21]. Let us pick an arbitrary face f_b, which we call the *boundary face*. We assume further that the vertices are ordered such that $v_1, v_2, \ldots, v_k$ are the vertices of f_b in cyclic order. An edge (vertex) is called *boundary edge (vertex)* if it lies on f_b, otherwise *interior edge (vertex)*. In this paper every embedding is considered as straight-line embedding. A 2d embedding of G is described by giving every vertex v_i a coordinate $\mathbf{p}_i = (x_i, y_i)^T$. We denote the 2d embedding with $G(\mathbf{p})$ and consider only embeddings that realize f_b as convex outer face.

The combination of the Maxwell-Cremona correspondence and barycentric embeddings provides an elegant technique for embedding 3-polytopes. Let us first define the common concept of both methods.

Definition 1 (Stress, Equilibrium) *An assignment $\omega \colon E \to \mathbb{R}$ of scalars to the edges of G (with $\omega(i,j) =: \omega_{ij} = \omega_{ji}$) is called a* stress. *Let $G(\mathbf{p})$ be a 2d embedding*

of G. A point $\mathbf{p}_i$ is in equilibrium, iff

$$\sum_{j:(i,j)\in E} \omega_{ij}(\boldsymbol{p}_i - \boldsymbol{p}_j) \;=\; \mathbf{0}. \tag{1}$$

The embedding of G is in equilibrium*, iff all of its points are in equilibrium.*

If $G(\mathbf{p})$ is in equilibrium according to ω, then ω is called *equilibrium stress* for $G(\mathbf{p})$. From special interest are stresses that are positive on every interior edge of G. These stresses are called *positive stresses.*

Suppose we fixed an embedding $G(\mathbf{p})$ in the plane. Let $h_i\colon V \to \mathbb{R}$ be a height assignment for the vertices of G. The function h defines a 3d embedding of G by giving every vertex $\mathbf{p}_i$ the additional z-coordinate $z_i = h(\mathbf{p}_i)$. If in the 3d embedding every face of G lies on a plane the height assignment h is called *lifting*. The so-called Maxwell-Cremona correspondence describes the following.

Theorem 1 (Maxwell [11], Whiteley). *Let G be a 3-connected planar graph with 2d embedding $G(\mathbf{p})$ and a designated face $\hat{f}$. There exists a correspondence between*

A.) equilibrium stresses ω on $G(\mathbf{p})$,
B.) liftings of $G(\mathbf{p})$ in $\mathbb{R}^3$, where face $\hat{f}$ lies in the xy-plane.

If the stress is positive, the lifting refers to a convex 3-polytope.

The complete proof of the Maxwell-Cremona correspondence is due to Whiteley [20] (see also [3]). Richter-Gebert's book [13, Section 13] containes a simple algorithm that computes the lifting: The location of every face in the lifting is specified by $G(\mathbf{p})$ and a plane on which the face lies. For convenience we introduce for every vertex $\mathbf{p}_i = (x_i, y_i)^T$ a (homogenized) 3d vertex $\mathbf{p}'_i := (x_i, y_i, 1)^T$. We define for every face f_j a vector $\mathbf{q}_j \in \mathbf{R}^3$, such that $\langle \mathbf{q}_j, \mathbf{p} \rangle$ describes the height of the point $\mathbf{p} \in f_j$ in the lifting. The vectors $\mathbf{q}$ can be computed incrementally by

$$\begin{aligned}
\mathbf{q}_b &= (0, 0, 0)^T, \\
\mathbf{q}_l &= \omega_{ij}(\mathbf{p}'_i \times \mathbf{p}'_j) + \mathbf{q}_r,
\end{aligned} \tag{2}$$

where the edge pointing from i to j, separates f_l and f_r, such that f_l lies to the left and f_r lies to the right. Notice that the computed lifting does not depend on the ordering of the faces that is used to determine the $\mathbf{q}$ vectors.

To apply the Maxwell-Cremona correspondence we need a 2d embedding of G with equilibrium stress. Let ω be an arbitrary stress that is zero on the boundary edges and positive on the interior edges. We obtain from the stress ω its *Laplace matrix $L = \{l_{ij}\}$*, which is defined by its entries as

$$l_{ij} := \begin{cases} -\omega_{ij} & \text{if } (i,j) \in E \text{ and } i \neq j, \\ \sum_j \omega_{ij} & \text{if } i = j, \\ 0 & \text{otherwise.} \end{cases}$$

An embedding $G(\mathbf{p})$ is described by the vectors $\mathbf{x} = (x_1, \ldots, x_n)^T$ and $\mathbf{y} = (y_1, \ldots, y_n)^T$. Let $B := \{1, \ldots, k\}$ and $I := \{k+1, \ldots, n\}$ be the index sets of the boundary, respectively interior vertices. We subdivide $\mathbf{x}, \mathbf{y}$, and L by B and I

and obtain $\mathbf{x}_B, \mathbf{x}_I, \mathbf{y}_B, \mathbf{y}_I, L_{BB}, L_{II}, L_{BI}$ and L_{IB}. The equilibrium condition (1) for the interior vertices can be phrased as $L_{IB}\mathbf{x}_B + L_{II}\mathbf{x}_I = \mathbf{0}$. The same holds for the y-coordinates. This implies that we can express the vectors $\mathbf{x}_I$ and $\mathbf{y}_I$ as linear functions in terms of $\mathbf{x}_B$ and $\mathbf{y}_B$, namely by

$$\mathbf{x}_I = -L_{II}^{-1}L_{IB}\mathbf{x}_B, \quad \mathbf{y}_I = -L_{II}^{-1}L_{IB}\mathbf{y}_B. \tag{3}$$

The matrix L_{II} is singular and hence the vectors $\mathbf{x}_I$ and $\mathbf{y}_I$ are properly and uniquely defined (see [13,7]). The embedding is known as (weighted) barycentric embedding. For every positive stress the coordinates give a strictly convex straight-line embedding (see for example [7]). A weighted barycentric embedding has the following nice interpretation: The interior edges of the graph can be considered as springs with spring constants ω_{ij}. The barycentric embedding models the equilibrium state of the system of springs when the boundary vertices are anchored at their fixed positions.

3 Extending an Equilibrium Stress to the Boundary

The interior vertices computed by (3) are in equilibrium by construction. However, the stressed edges of the boundary vertices do not sum up to zero but to

$$\forall i \in B \quad \sum_{j:(i,j)\in E} \omega_{ij}(\mathbf{p}_i - \mathbf{p}_j) \; =: \mathbf{F}_i. \tag{4}$$

To apply the Maxwell-Cremona correspondence we have to define the (yet unassigned) stresses on the boundary edges such that they cancel the vectors $\mathbf{F}_i$. If the outer face is a triangle this is always possible by solving a linear system with three unknowns [8]. But in general this is only possible for special locations of the boundary face. The problem how to position f_b is challenging, because changing the location of the boundary face will also change the vectors $\mathbf{F}_i$. We follow the approach of Ribó, Rote, and Schulz [12] to express this dependence and obtain a formalism that helps us to extend the equilibrium stress to the boundary.

Lemma 1 (Substitution Lemma [12]). *There are weights $\tilde{\omega}_{ij} = \tilde{\omega}_{ji}$, for $i, j \in B$, independent of location of the boundary face such that*

$$\forall i \in B \quad \mathbf{F}_i = \sum_{j\in B:j\neq i} \tilde{\omega}_{ij}(\mathbf{p}_i - \mathbf{p}_j). \tag{5}$$

The weights $\tilde{\omega}_{ij}$ are the off-diagonal entries of $-L_{BB} + L_{BI}L_{II}^{-1}L_{IB}$, which is the Schur Complement of L_{II} in L multiplied with -1.

Proof. Let $\mathbf{F}_x$ denote the vector $(F_1^x, \ldots, F_k^x)^T$, where F_i^x is the x-coordinate of the vector $\mathbf{F}_i$. We rephrase (4) as $\mathbf{F}_x = L_{BB}\mathbf{x}_B + L_{BI}\mathbf{x}_I$ and use (3) to substitute $\mathbf{x}_I$ to get

$$\mathbf{F}_x = L_{BB}\mathbf{x}_B - L_{BI}L_{II}^{-1}L_{IB}\mathbf{x}_B =: \tilde{L}\mathbf{x}_B.$$

The matrix $\tilde{L} = L_{BB} - L_{BI}L_{II}^{-1}L_{IB}$ is the Schur complement of L_{II} in L. For the y-coordinates, we obtain a similar formula with the same matrix $\tilde{L}$. We define

$\tilde{\omega}_{ij}$ as the off-diagonal entries $-\tilde{l}_{ij}$ of $\tilde{L}$. Since $L_{BI} = (L_{IB})^T$, the matrix $\tilde{L}$ is symmetric and therefore $\tilde{\omega}_{ij} = \tilde{\omega}_{ji}$ holds.

To show that the expression $\mathbf{F}_x = \tilde{L}\mathbf{x}_B$ has the form stated in (5) we have to check that all row sums in $\tilde{L}$ equal 0. Let $\mathbf{1}$ denote the vector where all entries are 1, equivalently $\mathbf{0}$ denotes the vector that contains only zeros as entries. Since each of the last $n - k$ rows of L sums up to 0, we have $L_{II}\mathbf{1} + L_{IB}\mathbf{1} = \mathbf{0}$; and hence $-L_{II}^{-1}L_{IB}\mathbf{1} = \mathbf{1}$. Plugging this expression into $\tilde{L}\mathbf{1} = L_{BB}\mathbf{1} - L_{BI}L^{-1}L_{IB}\mathbf{1}$ shows that $\tilde{L}\mathbf{1} = L_{BB}\mathbf{1} + L_{BI}\mathbf{1}$, which equals $\mathbf{0}$.   □

Notice that the $\tilde{\omega}$ values are independent of the location of the boundary face and depend only on the stress ω. From this point of view we can use the complete graph K_k on the boundary vertices with stress $\tilde{\omega}$ as substitution for the embedding $G(\mathbf{p})$ with stress ω to express the vectors $\mathbf{F}_i$. For this reason we call the stresses $\tilde{\omega}$ *substitution stresses*. With help of the substitution stresses we can simplify the problem how to locate the boundary face. A feasible position can be found by solving the non-linear system consisting of the $2k$ equations of (5) plus the $2k$ equations

$$\forall i \in B : \omega_{i,suc(i)}(\mathbf{p}_i - \mathbf{p}_{suc(i)}) + \omega_{i,pre(i)}(\mathbf{p}_i - \mathbf{p}_{pre(i)}) = -\mathbf{F}_i, \qquad (6)$$

where $suc(i)$ denotes the successor of v_i and $pre(i)$ denotes the predecessor of v_i on f_b in cyclic order. Since the equations are dependent the system is under-constrained. Later we fix some boundary coordinates to obtain a unique solution. An important property of the substitution stresses was observed in [12].

Lemma 2 ([12]). *If the stress ω is positive, then for every $i, j \in B$ the induced substitution stress $\tilde{\omega}_{ij}$ is positive.*

4   Constructing and Controlling an x-Equilibrium Stress

Let $x_1, \ldots, x_n$ be given as x-coordinates of $G(\mathbf{p})$. We are interested in a positive equilibrium stress that will give these x-coordinates in the barycentric embedding. In particular, we are looking for a positive stress ω such that

$$\forall i \in I \sum_{j:(i,j)\in E} \omega_{ij}(x_i - x_j) = 0. \qquad (7)$$

We call a positive stress that fulfills condition (7) a (positive) *x-equilibrium stress*. Since we consider in this paper only positive x-equilibrium stresses we omit the term "positive" in the following. As pointed out in [1], an x-monotone stress exists when every interior edge lies on some x-monotone path, whose endpoints are boundary vertices. Let us assume that we selected the x-coordinates such that the latter holds. Furthermore, we pick for every edge e some x-monotone path P_e.

We follow the approach of [1] to construct an x-monotone stress. The construction is based on assigning a cost $c_{\{i,j\}} > 0$ to every interior edge (i,j) of G. If the costs guarantee

$$\forall i \in I \sum_{j:(i,j)\in E:x_i<x_j} c_{\{i,j\}} = \sum_{(i,k)\in E:x_i>x_k} c_{\{i,k\}}, \qquad (8)$$

we can define an x-equilibrium stress by

$$\omega_{ij} = \frac{c_{\{i,j\}}}{|x_i - x_j|}. \tag{9}$$

We start with $c_{\{i,j\}} \equiv 0$ and increase the costs successively. Let $e = (i,j)$ be an edge with $c_{\{i,j\}} = 0$. We increase the costs of the edges of P_e by 1. In (8) both sides of the equation increase by 1 if v_i lies on P_e, otherwise nothing changes. Hence, (8) still holds. We repeat this procedure until every interior edge is assigned with a positive cost. The total cost for an edge is an integer smaller than $3n - 3$.

We show now how to modify an x-monotone stress to obtain helpful properties for the substitution stresses induced by ω. Our goal is to get a substitution stress that is maximal on an edge we picked. More precisely, let v_s and v_t be two non-incident vertices on the boundary of G and let $\alpha > 1$ be a constant that we fix later. The stress ω should guarantee that for all pairs of boundary vertices v_i, v_j we have $\tilde{\omega}_{st} > \alpha \tilde{\omega}_{ij}$, unless $\{i,j\} = \{s,t\}$. The idea how to achieve this is the following: We pick an x-monotone path P_{st} from v_s to v_t. Then we determine a suitable (large) number K and add K to the costs of every edge which is on P_{st}. The stress induced by the increased costs is still an x-equilibrium stress for our choice of x-coordinates. But if we think of the stresses as spring constants, we have increased the force that pushes v_s and v_t away from each other. Our hope is that this will reflect in the substitution stresses and makes $\tilde{\omega}_{st}$ the dominant stress.

First, let us bound all substitution stresses form above and then prove a lower bound for the stress $\tilde{\omega}_{st}$.

Lemma 3. *Let $L = \{l_{ij}\}$ be the Laplace matrix derived from a positive stress ω, and $\tilde{\omega}$ the corresponding substitution stress. For any $i,j \in B$ we have*

$$\tilde{\omega}_{ij} < \min\{l_{ii}, l_{jj}\}.$$

Proof. Since $\mathbf{u}^T L \mathbf{u} = \sum_{(i,j) \in E} \omega_{ij}(u_i - u_j)^2$, which is non-negative for any vector $\mathbf{u}$, the Laplace matrix is positive semidefinite. Let $\tilde{L} = \{\tilde{l}_{ij}\} = L_{BB} - L_{BI} L_{II}^{-1} L_{IB}$ denote the Schur complement of L_{II} in L. Due to [22, page 175] we know that $L_{II} - \tilde{L}$ is positive semidefinite. Therefore, all principal submatrices are positive semidefinite and we have $l_{ii} \geq \tilde{l}_{ii}$. As a consequence of the substitution lemma, we know that $\sum_{j \in B: i \neq j} \tilde{\omega}_{ij} = \tilde{l}_{ii}$, and hence $\sum_{j \in B: i \neq j} \tilde{\omega}_{ij} \leq l_{ii}$. Since each of the $\tilde{\omega}_{ij}$'s is positive, each summand has to be smaller than l_{ii}. By the same argument we can show that $\tilde{\omega}_{ij} \leq l_{jj}$ and the lemma follows. $\square$

The next lemma proves a lower bound for $\tilde{\omega}_{st}$ and determines the number K that guarantees that $\tilde{\omega}_{st}$ becomes the dominant stress.

Lemma 4. *Let ω be an x-equilibrium stress obtained from the edge costs $c_{\{i,j\}}$ for $x_1, \ldots, x_n$ that is increased along an x-monotone path from v_s to v_t, by increment-ing the edge costs for edges on the path by K. The substitution stresses and the matrix L are obtained from ω as usual. Then*

$$\tilde{\omega}_{st} > \frac{K - 3n^2(1 + (k-2)\Delta_x)}{x_t - x_s},$$

where k denotes the number of boundary vertices and Δ_x the largest distance between two x-coordinates. Let $\alpha > 0$ be a parameter that will be fixed later. For $K \geq 3n^2(1 + (\alpha + k - 2)\Delta_x)$ we obtain for any $\tilde{\omega}_{ij}$ that is not $\tilde{\omega}_{st}$

$$\tilde{\omega}_{st} > \alpha\tilde{\omega}_{ij}.$$

Proof. Before bounding $\tilde{\omega}_{st}$ we show an upper bound for the other substitution stresses. Let $\tilde{\omega}_{ij}$ be such a stress. By Lemma 3, $\tilde{\omega}_{ij}$ is less than l_{rr} ($r \in \{i,j\} \cap \{s,t\}$). Since l_{rr} is a diagonal entry of the Laplace matrix it equals $\sum_{k:(r,k)\in E} \omega_{rk}$, which is a sum of at most $n - 1$ summands. We can assume that the path P_{st} uses no boundary edge. In this case each summand in $\sum_{k:(r,k)\in E} \omega_{rk}$ is smaller than $3n - 3$ and we obtain

$$\forall ij \neq st \quad \tilde{\omega}_{ij} < \max_{r \in B \setminus \{s,t\}} \{l_{rr}\} < 3n^2. \tag{10}$$

Let F_t^x be the x-component of $\mathbf{F}_t$. We combine (10) and (5) and obtain as upper bound for F_t^x

$$\tilde{\omega}_{st}(x_t - x_s) + (k-2)3n^2\Delta_x > F_t^x.$$

On the other hand we can express F_t^x by (4). The cost of one edge (k,t), with $x_k < x_t$, was increased by K. All other costs are in total less than $3n^2$. Thus,

$$F_t^x = \sum_{k:(k,t)\in E} \omega_{kt}(x_t - x_k) = \sum_{\substack{k:x_k < x_t \\ (k,t)\in E}} c_{\{t,k\}} - \sum_{\substack{k:x_k > x_t \\ (k,t)\in E}} c_{\{t,k\}} > K - 3n^2.$$

Combining the two bounds for F_t^x leads to the bound for $\tilde{\omega}_{st}$ stated in the lemma. Setting $K \geq 3n^2(1 + (\alpha + k - 2)\Delta_x)$ yields

$$\tilde{\omega}_{st} > \frac{3n^2(\alpha + k - 2)\Delta_x - 3n^2(k-2)\Delta_x}{x_t - x_s} = \frac{3n^2\alpha\Delta_x}{x_t - x_s} \geq 3n^2\alpha > \alpha\tilde{\omega}_{ij}.$$

□

As last part of this section we show that we can even enforce a set of substitution stresses to be dominant. Let v_{t_1}, v_{t_2} be two vertices that are both nonincident to v_s and let $x_{t_1} = x_{t_2}$. We can increment a given x-equilibrium stress by first increasing the edge costs $c_{\{i,j\}}$ along an x-monotone path from v_s to v_{t_1} by K and then do the same for an appropriate path from v_s to v_{t_2}.

Lemma 5. *Assume the same as in Lemma 4, but this time consider two paths: from v_s to v_{t_1} and from v_s to v_{t_2}. Assume further that $x_{t_1} = x_{t_2}$. For $K \geq 3n^2(1 + (\alpha + k - 2)\Delta_x)$ we have for any $\tilde{\omega}_{ij}$ with $\{i,j\} \not\subset \{s, t_1, t_2\}$*

$$\tilde{\omega}_{st_1} > \alpha\tilde{\omega}_{ij}, \quad \text{and} \quad \tilde{\omega}_{st_2} > \alpha\tilde{\omega}_{ij}.$$

Proof. Lemma 4 relies on the fact that we can bound $\sum_{j \neq s} \tilde{\omega}_{jt}(x_t - x_j)$ because by (10) the $\tilde{\omega}$'s in this sum are small. We cannot use this bound for $\tilde{\omega}_{t_1 t_2}(x_{t_1} - x_{t_2})$ anymore, but this summand cancels anyway, since $x_{t_1} = x_{t_2}$. Following the steps of the proof of Lemma 4 with first choosing $t = t_1$ and then choosing $t = t_2$ shows the lemma. □

Notice that the bounds for K are very rough. Better bounds can be obtained easily, but they would have a more complicated expression. Since for our purpose the fact that we can always find a valid number K is more important than the actual size of K, we presented a simple bound for K.

5   The Embedding Algorithm

5.1   The Algorithm Template

In this section we present as main result of this paper

Theorem 2. *Let G be a 3-connected planar graph. G admits an embedding as 3-polytope inside a $2(n-2) \times 2 \times 1$ box under the vertex resolution rule.*

We prove Theorem 2 by introducing an algorithm that constructs the desired embedding. The number of vertices on the boundary face plays an important role. The smaller this number is, the simpler is it to construct an embedding. For this reason we choose as boundary face f_b the smallest face of G. Due to Euler's formula f_b has at most 5 vertices. Depending on the size of f_b we obtain three versions of the algorithm which all follow the same basic pattern.

Our goal is to construct a planar embedding of G that has a positive stress and whose x-coordinates are distinct integers. The corresponding lifting of such an embedding fulfills the vertex resolution rule independently of its y and z-coordinates. Hence, we can scale in direction of the y and z-axis without violating the vertex resolution rule. The basic procedure is summarized in Algorithm 5.1.

Algorithm 1 Embedding algorithm as template.

1: Choose the x-coordinates.
2: Construct an x-equilibrium stress ω.
3: Choose the boundary y-coordinates.
4: Embed G as barycentric embedding with stress ω in the plane.
5: Lift the plane embedding.

Steps 1,4, and 5 are mostly independent of the size of f_b and will be discussed first. We start with some strictly convex plane embedding of G – called pre-embedding. Let $\hat{x}_1, \ldots, \hat{x}_n$ and $\hat{y}_1, \ldots, \hat{y}_n$ be the coordinates of the pre-embedding which we compute as barycentric embedding. We assume that in the pre-embedding all x-coordinates are different. If this is not the case we can perturb the stresses of the (pre-)embedding to achieve this. Since the pre-embedding is strictly convex [19] every edge lies on some x-monotone path. As done in Section 4, we fix for every interior edge e such a path P_e. The x-coordinates of the pre-embedding induce a strict linear order on the vertices of G. We denote with b_i the number of vertices with smaller x-coordinate compared to v_i in the pre-embedding. The x-coordinates of the (final) embedding are defined as $x_i := b_i$. Thus, no two vertices get the same x-coordinate and the largest x-coordinate is less than n. We observe that the paths P_e remain x-monotone. Therefore, they can be used to define an appropriate x-equilibrium stress ω. For technical reasons we might choose the same x-coordinate for some of the boundary vertices. In this case we check the vertex resolution rule for these vertices in the final embedding by hand. Step 4 and 5 can be realized as straight-forward implementations of the barycentric embedding and Maxwell's lifting. Notice that the value of the (extended) stress on the boundary edges is not needed to compute the lifting, because we can place an interior face in the xy-plane and then compute the lifting using only interior edges.

Steps 2 and 3 are the difficult parts of the algorithm. We have to choose the stress ω and the y-coordinates such that an extension of the stress to the boundary is possible. Moreover, the boundary coordinates have to yield a convex boundary face. We continue with the three different cases and discuss step 2 and 3 of the algorithm template for each of them separately.

5.2   Graphs with Triangular Face

The case where f_b is a triangle is the easiest case because we can extend every stress to the boundary for every location of the outer face (see Section 3). This case was already addressed by Chrobak, Goodrich and Tamassia [1]. The discussion in this section will prove the following statement:

Proposition 1. *Let G be a 3-connected planar graph and let G contain a triangular face. G admits an embedding as 3-polytope inside an $(n-1) \times 1 \times 1$ box under the vertex resolution rule.*

Let us compute the pre-embedding with the boundary coordinates $x_1 = 0, x_2 = 1$, and $x_3 = 0$. We use the x-monotone paths P_e to compute a suitable x-equilibrium stress ω as discussed in Section 4. Next we compute the barycentric embedding with boundary coordinates $\mathbf{p}_1 = (0,0)^T, \mathbf{p}_2 = (n-1,0)^T$, and $\mathbf{p}_3 = (0,1)^T$. As result we obtain interior y-coordinates in the interval $(0,1)$. Any two vertices have distance at least 1, since their x-coordinates differ by at least 1. (This is not true for v_1 and v_3, but their distance is $y_3 - y_1 = 1$.)

5.3   Graphs with Quadrilateral Face

Let us assume now that G contains a quadrilateral but no triangular face. In this case it is not always possible to extend an equilibrium stress ω to the boundary. The observations of Section 3 help us to overcome this difficulty. We use as boundary coordinates for the pre-embedding $\hat{x}_1 = 0, \hat{x}_2 = 1, \hat{x}_3 = 1$, and $\hat{x}_4 = 0$. The x-coordinates induced by the pre-embedding give $x_2 = x_3 = n - 2$. We redefine the boundary x-coordinates by setting $x_2 = n - 2$ and $x_3 = 2(n - 2)$. Notice that this preserves the x-monotonicity of the paths P_e, but makes it easier to extend the stress to the boundary as we will see in the following.

Let ω be the x-monotone stress for the obtained x-coordinates. We can express the influence of the stressed edges of G on the boundary with help of the substitution stresses $\tilde{\omega}$. We modify ω with the technique described in Lemma 4 to assure that $\tilde{\omega}_{13} > \tilde{\omega}_{24}$. Let us now discuss how to extend the stress ω to the boundary. To solve the non-linear system given by (5) and (6) we fix some of the boundary y-coordinates to obtain a unique solution. In particular, we set $y_1 = 0, y_2 = 0$, and $y_4 = 1$. As final coordinate we obtain[1]

$$y_3 = \frac{\tilde{\omega}_{24}}{2\tilde{\omega}_{13} - \tilde{\omega}_{24}}.$$

Since $\tilde{\omega}_{13} > \tilde{\omega}_{24}$, we can deduce that $0 < y_3 < 1$. Hence, all y-coordinates are contained in $[0,1]$. Furthermore, we know that the only two vertices with the same

---

[1] The solution of the non-linear system was obtained by computer algebra software.

x-coordinate, namely v_1 and v_4, have the distance $y_4 - y_1 = 1$. Therefore the vertex resolution rule holds. If we scale the induced lifting such that the largest z-coordinate equals 1 we obtain:

Proposition 2. *Let G be a 3-connected planar graph and let G contain a quadrilateral face. G admits an embedding as 3-polytope inside a $2(n-2) \times 1 \times 1$ box under the vertex resolution rule.*

5.4   The General Case

The most complicated case is the case where we have to use a pentagon as boundary face. However, the basic pattern how to construct the embedding remains the same. We choose as x-coordinates for the pre-embedding $\hat{x}_1 = 0, \hat{x}_2 = 1, \hat{x}_3 = 1, \hat{x}_4 = 0$, and $\hat{x}_5 = -\varepsilon$, for $\varepsilon > 0$ small enough to guarantee that all interior vertices get a positive x-coordinate in the pre-embedding. We change the induced x-coordinates on the boundary without changing the monotonicity of the paths P_e. In particular, we set $x_1 = 0, x_2 = n - 2, x_3 = n - 2, x_4 = 0$, and $x_5 = -(n - 2)$. The stress ω is constructed such that the substitution stresses guarantee

$$\tilde{\omega}_{25} > 3\tilde{\omega}_{13}, \tilde{\omega}_{25} > 3\tilde{\omega}_{14}, \tilde{\omega}_{25} > 3\tilde{\omega}_{24}, \tilde{\omega}_{35} > 3\tilde{\omega}_{13}, \tilde{\omega}_{35} > 3\tilde{\omega}_{14}, \tilde{\omega}_{35} > 3\tilde{\omega}_{24}. \quad (11)$$

In other words the substitution stresses $\tilde{\omega}_{25}$ and $\tilde{\omega}_{35}$ dominate all other substitution stresses on interior edges by a factor 3. Since $x_3 = x_2$, we can construct a stress ω that induces a substitution stress that fulfills (11) by the observations of Lemma 5.

Appropriate boundary y-coordinates can be obtained by solving the non-linear system given by (5) and (6). As done in the previous case we fix some y-coordinates to obtain a unique solution. This time we set $y_1 = -1, y_4 = 1$, and $y_5 = 0$. This yields for the two remaining y-coordinates

$$y_2 = -2 - 2\frac{\tilde{\omega}_{24}\tilde{\omega}_{13} - \tilde{\omega}_{13}^2 - \tilde{\omega}_{35}\tilde{\omega}_{14} - 2\tilde{\omega}_{13}\tilde{\omega}_{35}}{\tilde{\omega}_{24}\tilde{\omega}_{35} + \tilde{\omega}_{25}\tilde{\omega}_{13} + 2\tilde{\omega}_{25}\tilde{\omega}_{35}},$$

$$y_3 = \quad 2 + 2\frac{\tilde{\omega}_{24}\tilde{\omega}_{13} - \tilde{\omega}_{24}^2 - \tilde{\omega}_{14}\tilde{\omega}_{25} - 2\tilde{\omega}_{24}\tilde{\omega}_{25}}{\tilde{\omega}_{24}\tilde{\omega}_{35} + \tilde{\omega}_{25}\tilde{\omega}_{13} + 2\tilde{\omega}_{25}\tilde{\omega}_{35}}.$$

We have to check two things: f_b has to be convex and $y_3 - y_2$ should be large enough to guarantee the vertex resolution rule. First we show that $-2 < y_2$ and $y_3 < 2$, which would imply that f_b is convex if $y_3 > y_2$. The inequalities $-2 < y_2$ and $y_3 < 2$ hold, iff

$$\tilde{\omega}_{24}\tilde{\omega}_{13} - \tilde{\omega}_{13}^2 - \tilde{\omega}_{35}\tilde{\omega}_{14} - 2\tilde{\omega}_{35}\tilde{\omega}_{13} < 0 \text{ and}$$
$$\tilde{\omega}_{24}\tilde{\omega}_{13} - \tilde{\omega}_{24}^2 - \tilde{\omega}_{14}\tilde{\omega}_{25} - 2\tilde{\omega}_{25}\tilde{\omega}_{24} < 0.$$

Both inequalities are true, because as a consequence of (11) the only positive summand $\tilde{\omega}_{24}\tilde{\omega}_{13}$ is smaller than $\tilde{\omega}_{35}\tilde{\omega}_{13}$ and smaller than $\tilde{\omega}_{25}\tilde{\omega}_{24}$. The difference $y_3 - y_2$ equals

$$4 + 2\frac{2\tilde{\omega}_{24}\tilde{\omega}_{13} - \tilde{\omega}_{13}^2 - \tilde{\omega}_{24}^2 - \tilde{\omega}_{35}(\tilde{\omega}_{14} + 2\tilde{\omega}_{13}) - \tilde{\omega}_{25}(\tilde{\omega}_{14} + 2\tilde{\omega}_{24})}{\tilde{\omega}_{24}\tilde{\omega}_{35} + \tilde{\omega}_{25}\tilde{\omega}_{13} + 2\tilde{\omega}_{25}\tilde{\omega}_{35}}.$$

Due to (11) we know that $\tilde{\omega}_{14} + 2\tilde{\omega}_{24} < \tilde{\omega}_{35}$ and $\tilde{\omega}_{14} + 2\tilde{\omega}_{13} < \tilde{\omega}_{25}$. Thus

$$y_3 - y_2 > 4 + 2\frac{2\tilde{\omega}_{24}\tilde{\omega}_{13} - \tilde{\omega}_{13}^2 - \tilde{\omega}_{24}^2 - 2\tilde{\omega}_{35}\tilde{\omega}_{25}}{\tilde{\omega}_{24}\tilde{\omega}_{35} + \tilde{\omega}_{25}\tilde{\omega}_{13} + 2\tilde{\omega}_{25}\tilde{\omega}_{35}} > 2.$$

The estimation holds since (again due to (11)) $\tilde{\omega}_{24}\tilde{\omega}_{35} > \tilde{\omega}_{24}^2$ and $\tilde{\omega}_{25}\tilde{\omega}_{13} > \tilde{\omega}_{13}^2$, and hence the fraction is greater -1.

We multiply all y-coordinates by $1/2$. This yields $y_4 - y_1 = 1$ and $y_3 - y_2 > 1$. The z-coordinates are scaled such that they lie between 0 and 1. Clearly, the vertex resolution rule holds for the computed embedding.

We finish this section with some remarks on the running time of the embedding algorithm. As mentioned in [1] the x-monotone stress can be computed in linear time. The barycentric embedding (which we use twice, once for the pre-embedding and once for the intermediate plane embedding) can be computed by the linear system (3). Since the linear system is based on a planar structure, it can be solved with nested dissections (see [9,10]) based on the planar separator theorem. As a consequence a solution can be computed in $O(M(\sqrt{n}))$ time, where $M(n)$ is the upper bound for multiplying two $n \times n$ matrices. The current record for $M(n)$ is $O(n^{2.325})$, which is due to Coppersmith and Winograd [2]. The computation of the lifting can be done in linear time. In total, we achieve a running time of $O(n^{1.1625})$.

6   Additional Properties of the Embedding

6.1   Induced Grid Embedding

Besides the small embedding under the vertex resolution rule, the constructed embedding has several other nice properties which we discuss in this section. Since the computed y and z-coordinates are expressed by a linear system of rational numbers, they are rational numbers as well. Thus, we can scale the final embedding to obtain a grid embedding. We first prove a technical lemma.

Lemma 6. *Suppose that all x and y-coordinates as well as all stresses ω are integers. Let the difference between two x-coordinates be less than Δ_x and let the difference between two y-coordinates be less than Δ_y. Then the height z_i of any point $\mathbf{p}_i$ in the lifting is an integer and it can be bounded by*

$$0 \leq z_i \leq |\omega_{12}| \cdot \Delta_x \cdot \Delta_y,$$

where ω_{12} is a stress on an arbitrary boundary edge.

Proof. Since by (2) all heights can be expressed as additions and multiplications of integers, the heights are integral. Moreover, all heights are invariant under rigid motions of the plane embedding. Hence, we can assume that $y_1 = y_2 = 0$, $x_1 = 0$, and and all y-coordinates are nonnegative. The lifted polytope lies between the planes that contain the faces adjacent to the edge $(1, 2)$. One of these faces is the face f_b, which lies in the plane $z = 0$. Let the other face be f_1. We denote by $\mathbf{p}_{max}$ the vertex that attains the maximal height z_{max} in the lifting. For the homogenized vertex $\mathbf{p}'_{max}$ we have $\langle \mathbf{p}'_{max}, \mathbf{q}_1 \rangle \geq z_{max}$. Due to (2) $\mathbf{q}_1 = \omega_{12}(0, -x_2, 0)^T$, and hence $|\omega_{12}| \cdot \Delta_x \cdot \Delta_y \geq \langle \mathbf{p}'_{max}, \mathbf{q}_1 \rangle$ and the lemma follows.   □

Theorem 3. *The embedding computed with Algorithm 5.1 can be scaled to integer coordinates such that*

$$\begin{aligned} 0 &\leq& x_i &\leq& 2(n-2), \\ 0 &\leq& y_i, z_i &\leq& 2^{O(n^2 \log n)}. \end{aligned}$$

Proof. We analyze the case where the boundary face is a pentagon. Convince yourself that this case needs in fact the largest grid. We multiply the computed stress ω by $n!$ and obtain an integral stress ω'. Let L' be the Laplace matrix induced by the scaled stress. The substitution stresses $\tilde{\omega}$ are defined as off diagonal entries of $L'_{BI} L'_{II}{}^{-1} L'_{IB}$. Since we have integral stresses ω' the entries of L' are integral as well. Due to the adjoint formula for the inverse of a matrix, the substitution stresses are rational numbers and multiples of $1/\det L'_{II}$.

The y-coordinates of the embedding are computed by $\mathbf{y}_I = -L_{II}^{-1} L_{IB} \mathbf{y}_B$. We multiply the vector $\mathbf{y}_B$ by $(\tilde{\omega}_{24}\tilde{\omega}_{35} + \tilde{\omega}_{25}\tilde{\omega}_{13} + 2\tilde{\omega}_{25}\tilde{\omega}_{35})(\det L'_{II})^2$ to make it integral. Notice that scaling the stress leaves the barycentric embedding unchanged. Due to Cramer's rule and (3) we have for every interior vertex v_i

$$ y_i = \frac{\det L'_{II}(i)}{\det L'_{II}}, $$

where $L'_{II}(i)$ denotes the matrix L'_{II} with row i substituted by $\mathbf{y}_B$. Since $\det L'_{II}(i)$ is integral the interior y-coordinates are multiples of $1/\det L'_{II}$. Thus multiplying $\mathbf{y}_B$ (again) by $\det L'_{II}$ gives integer y-coordinates. In total we scale by $(\tilde{\omega}_{24}\tilde{\omega}_{35} + \tilde{\omega}_{25}\tilde{\omega}_{13} + 2\tilde{\omega}_{25}\tilde{\omega}_{35})(\det L'_{II})^3$, which is clearly dominated by $(\det L'_{II})^3$. Let us now discuss how to bound $\det L'_{II}$. Since L' is positive semidefinite, L'_{II} as principal submatrix is positive semidefinite as well. Therefore, we can bound the determinant by Hadarmard's inequality (see [22, page 176]) and obtain

$$ \det L'_{II} \leq \prod_{i=4}^{n} l'_{ii}. $$

Each entry l'_{ii} equals the sum of stresses ω' incident to v_i. Without scaling the stresses are in $O(n^3)$ (a rough estimation gives $K \leq 42n^3 + 3n^2$). Hence, every stress ω'_{ij} is in $O(n!)$ and so is l'_{ii}. This implies that $(\det L'_{II})^3$ is bounded by $2^{O(n^2 \log n)}$.

We continue with the analysis of the lifting with help of Lemma 6. Let us first discuss how to bound ω_{12}. Remember that the x-monotone stress was constructed by incrementing costs on some x-monotone paths. Instead of considering x-monotone paths one can use cycles to define the appropriate stresses. Such a cycle consists of the old x-monotone path and closes this path by a path over the boundary. The x-monotone increasing path of the cycle adds a $+1$ to the total costs of its edges – the x-monotone decreasing path adds a -1 to the costs of its edges. Notice that we have to route only one of the cycles via the edge $(1, 2)$. This implies that $\omega'_{12} = -n!/|x_1 - x_2|$. Applying Lemma 6 leads to the bound for the largest z-coordinate of $O(n! \cdot 2n \cdot (\det L'_{II})^3) = 2^{O(n^2 \log n)}$. □

Compared to the grid embedding presented in [12], we were able to reduce the size of the x-coordinates (from $2n \cdot 8.107^n$ to $2(n-2)$) at the expense of the y and z-coordinates.

6.2 Spread of the Embedding

The *spread* of a point set is the quotient of the longest pairwise distance (the diameter) and the shortest pairwise distance. The smaller this ratio is, the more

densely the point set is packed. A small spread implies that the points are "evenly distributed". We define as *spread of an embedding of a polytope* the spread of its points.

Theorem 4. *The spread of a 3-polytope embedded by Algorithm 5.1 is smaller than $2n$. There are infinitely many polytopes without an embedding with spread smaller than $(n-1)/\pi$.*

Proof. Let us first analyze the spread of the constructed 3-polytope. The diameter of its point set depends on the size of the boundary face. It can be checked that in all cases it is smaller than $2n$. Since the smallest distance is larger than 1 the spread is less than $2n$.

We discuss now how large the spread of a 3-polytope can be. We assume that the embedding is scaled such that the smallest pointwise distance equals 1. Let G be the graph of a 3-dimensional pyramid. In any realization as 3-polytope the perimeter of its $(n-1)$-gonal base is larger than $n-1$. Since for convex sets the perimeter is smaller π times the diameter [17], we have that the spread of the $(n-1)$-gon (and hence the spread of the pyramid) is larger than $(n-1)/\pi$. □

Notice that in the 2d setting the points of the intermediate plane embedding of G have also a spread smaller than n. Following the arguments of the proof of Theorem 4, a convex drawing of an n-gon needs a point set of spread n/π. Thus, for convex 2d drawings, the intermediate plane embedding of our algorithm has a spread that differs from the best possible only by a constant multiplicative factor.

7   An Example

We show as example how to realize a dodecahedron with help of Algorithm 5.1. The graph G of the dodecahedron is particular suitable for a good example, because every face of G is a pentagon. Thus we have to apply the more complicated part of the algorithm. Due to the symmetry of G it does not matter which face we select as the boundary face. We follow our convention and name the vertices such that $\mathbf{p}_1, \ldots, \mathbf{p}_5$ belong to f_b in cyclic order.

We start with a plane drawing (the pre-embedding) of G with strictly convex faces and no vertical edges. Figure 1 shows our choice. The pre-embedding induces an ordering of the vertices which we use to define the x-coordinates, namely

$$\mathbf{x} = (0, 18, 18, 0, -18, 6, 3, 12, 13, 11, 15, 4, 7, 17, 14, 16, 5, 9, 10, 8)^T.$$

Notice that the boundary x-coordinates are selected according to the algorithm. Next we construct the stress ω. We select some x-monotone paths and compute the induced costs for the interior edges. The stresses ω induce the matrix $\tilde{L}$ which includes the substitution stresses as off-diagonal entries (multiplied with -1). In our example we obtain

$$\tilde{L} = \begin{pmatrix} 0.234791 & -0.0769685 & -0.0815444 & -0.0354125 & -0.0408658 \\ -0.0769685 & 0.410969 & -0.264196 & -0.0401058 & \mathbf{-0.02969} \\ -0.0815444 & -0.264196 & 0.506504 & -0.108953 & \mathbf{-0.05181} \\ -0.0354125 & -0.0401058 & -0.108953 & 0.215884 & -0.031412 \\ -0.0408658 & \mathbf{-0.02969} & \mathbf{-0.05181} & -0.031412 & 0.153786 \end{pmatrix}.$$
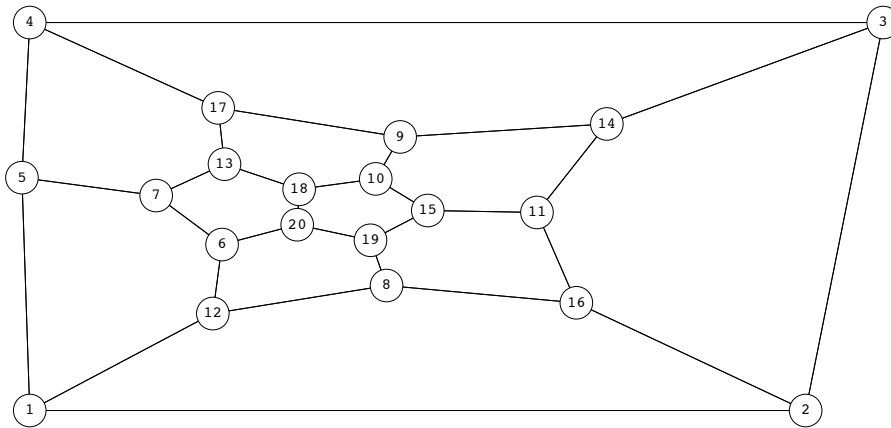
Fig. 1. The pre-embedding of the dodecahedron.

It can be observed, that the entries $\tilde{l}_{35}$ and $\tilde{l}_{25}$ are not the dominating entries. But for the correctness of the algorithm this is needed. Indeed, for our choice of substitution stresses right now, we would obtain the embedding shown in Figure 2(a). The figure illustrates that the too small substitution stresses $\tilde{\omega}_{25}$ and $\tilde{\omega}_{35}$ cause a non-convex boundary face f_b. Fortunately, we can fix the problem by picking two


(a)   (b)
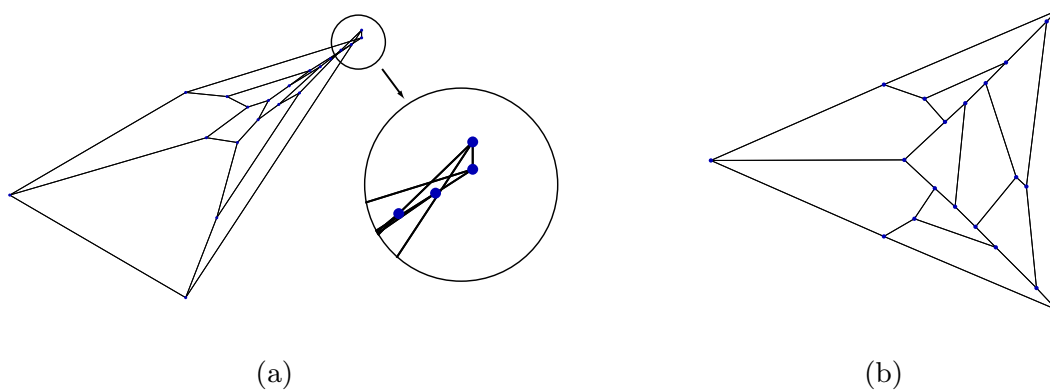
Fig. 2. Embedding without (a) and with (b) making $\tilde{\omega}_{25}$ and $\tilde{\omega}_{35}$ dominant.

x-monotone paths P_{25} and P_{35} and increment the costs on its edges by K. We choose K according to Lemma 5. Since in our case $n = 20$, $\Delta x = 36$, and $k = 5$, it suffices to set $K = 260\,400$ (notice that we need to pick $\alpha = 3$). The modified

stress ω gives now

$$\tilde{L} = \begin{pmatrix} 0.319465 & -0.151322 & -0.0666023 & -0.00126453 & -0.100277 \\ -0.151322 & 7.1641 & -2.97443 & -0.0515457 & -\mathbf{3.9868} \\ -0.0666023 & -2.97443 & 7.22698 & -0.144387 & -\mathbf{4.04156} \\ -0.00126453 & -0.0515457 & -0.144387 & 0.275482 & -0.0782853 \\ -0.100277 & -\mathbf{3.9868} & -\mathbf{4.04156} & -0.0782853 & 8.20693 \end{pmatrix}.$$

We observe that both $\tilde{\omega}_{35}$ and $\tilde{\omega}_{25}$ are greater than $3\tilde{\omega}_{14}$, $3\tilde{\omega}_{24}$ and $3\tilde{\omega}_{13}$. Therefore, we can continue with the algorithm and choose $\mathbf{y}_B$ as described in Section 5.4. The induced barycentric embedding is shown in Figure 2(b) and the corresponding lifting is depicted in Figure 3(a). We did not execute the final scaling to obtain a more illustrative picture. Notice that every face is still drawn as strictly convex polygon. However, since we chose the value for K that high some faces become almost collinear. A more "spherical" embedding could be obtained by lowering the value for K and check if this leaves $y_3 - y_2 > 1$. Such a drawing (for $K = 10$) is shown in Figure 3(b).

(a)   (b)
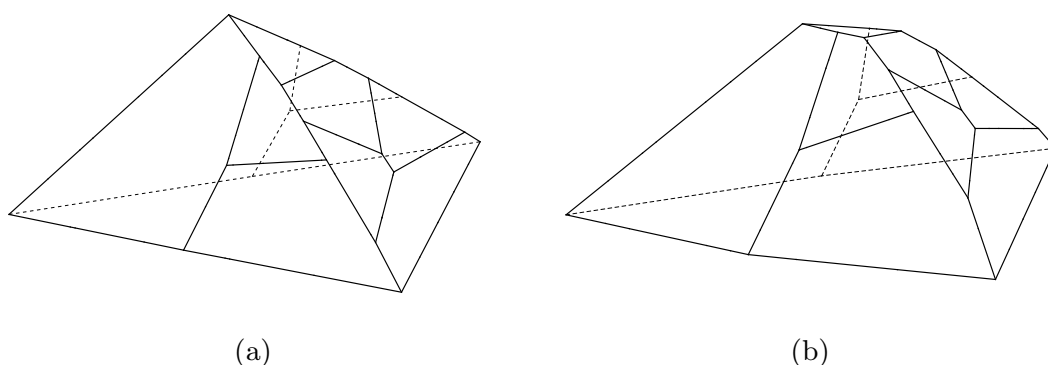
Fig. 3. The final embedding (a) and the induced embedding for $K = 10$ (b).

References

1. M. Chrobak, M. T. Goodrich, and R. Tamassia. Convex drawings of graphs in two and three dimensions (preliminary version). In *12th Symposium on Computational Geometry*, pages 319–328, 1996.
2. D. Coppersmith and S. Winograd. Matrix multiplication via arithmetic progressions. *J. Symb. Comput.*, 9(3):251–280, 1990.
3. H. Crapo and W. Whiteley. Plane self stresses and projected polyhedra I: The basic pattern. *Structural Topology*, 20:55–78, 1993.
4. G. Das and M. T. Goodrich. On the complexity of optimization problems for 3-dimensional convex polyhedra and decision trees. *Comput. Geom. Theory Appl.*, 8(3):123–137, 1997.
5. H. de Fraysseix, J. Pach, and R. Pollack. How to draw a planar graph on a grid. *Combinatorica*, 10(1):41–51, 1990.

6. P. Eades and P. Garvan. Drawing stressed planar graphs in three dimensions. In F.-J. Brandenburg, editor, *Graph Drawing*, volume 1027 of *Lecture Notes in Computer Science*, pages 212–223. Springer, 1995.

7. S. J. Gortler, C. Gotsman, and D. Thurston. Discrete one-forms on meshes and applications to 3d mesh parameterization. *Computer Aided Geometric Design*, 23(2):83–112, 2006.

8. J. E. Hopcroft and P. J. Kahn. A paradigm for robust geometric algorithms. *Algorithmica*, 7(4):339–380, 1992.

9. R. J. Lipton, D. Rose, and R. Tarjan. Generalized nested dissection. *SIAM J. Numer. Anal.*, 16(2):346–358, 1979.

10. R. J. Lipton and R. E. Tarjan. Applications of a planar separator theorem. *SIAM J. Comput.*, 9(3):615–627, 1980.

11. J. C. Maxwell. On reciprocal figures and diagrams of forces. *Phil. Mag. Ser.*, 27:250–261, 1864.

12. A. Ribó Mor, G. Rote, and A. Schulz. Small grid embeddings of 3-polytopes. submitted for publication, `http://arxiv.org/abs/0908.0488`, 2009.

13. J. Richter-Gebert. *Realization Spaces of Polytopes*, volume 1643 of *Lecture Notes in Mathematics*. Springer, 1996.

14. W. Schnyder. Embedding planar graphs on the grid. In *Proc. 1st ACM-SIAM Sympos. Discrete Algorithms*, pages 138–148, 1990.

15. O. Schramm. Existence and uniqueness of packings with specified combinatorics. *Israel J. Math.*, 73:321–341, 1991.

16. A. Schulz. *Lifting planar graphs to realize integral 3-polytopes and topics in pseudo-triangulations*. PhD thesis, Free University Berlin, 2008.

17. P. R. Scott and P. W. Awyong. Inequalities for convex sets. *J. Ineq. Pure and Appl. Math.*, 1(1), 2000.

18. E. Steinitz. Encyclopädie der mathematischen Wissenschaften. In *Polyeder und Raumteilungen*, pages 1–139. 1922.

19. W. T. Tutte. How to draw a graph. *Proceedings London Mathematical Society*, 13(52):743–768, 1963.

20. W. Whiteley. Motion and stresses of projected polyhedra. *Structural Topology*, 7:13–38, 1982.

21. H. Whitney. A set of topological invariants for graphs. *Amer. J. Math.*, 55:235–321, 1933.

22. F. Zhang. *Matrix Theory*. Springer, 1999.